A Unified Model of Thalamocortical Axon Guidance

Jean-Philippe Thivierge, Thomas R. Shultz & Evan Balaban
Department of Psychology, McGill University

Abstract

Thalamocortical (TC) projections project through the ventral telencephalon (VTe) to relay sensory information from the thalamus (Th) to the neocortex (NC). Information comes into the Th regionally segregated by sensory modality (vision, hearing, touch), and within each modality, by body region; the TC projections conserve the topography both by modality (sent to different brain regions [inter-area]) and body region (within each brain region [intra-area]). Initial TC projections are established by an activity-independent process that includes the gradient expression of Eph/ephrin molecules. Subsequently, an activity-dependent process working through synaptic depolarization refines the position of axons in the NC. We propose a model that combines activity-independent servomechanical guidance of TC axons and competitive mechanisms preventing spatial clustering of axons with an activity-dependent, Hebbian winner-take-all process (based on the activation of NMDA and GABA receptors) used in previous work (Thivierge & Balaban, 2005). This model governs both initial projections from the thalamus to the VTe, and subsequent movement of axons from the VTe to target regions of the NC, and reproduces the both inter-regional and intra-regional topography of TC projections. Simulations replicate experiments with ephrin-A5 knockout mice as well as cortical reorganization following focal deafferentation. The model is the first to integrate both activity-independent and activity-dependent processes to explain cortical map formation, and yields testable predictions for future experiments.

1. Introduction

Executing and monitoring appropriate behaviors requires that sensory information be processed and integrated efficiently. Thalamocortical (TC) projections relay information from the thalamus to the cerebral cortex in a highly ordered fashion: information from different senses is initially processed in separate cortical areas, and within each area, information is organized according to the spatial arrangement of the sensory receptors on the body surface – so-called topographic (retinotopic, somatotopic and cochleotopic[tonotopic]) maps. Sensory information from sensors within muscles and tendons also needs to be brought to motor-related areas of the cortex. During embryonic and early postnatal development, TC projections from the thalamus (ventrobasal nucleus of the thalamus; Th) reach target sites in the neocortex (NC). In this process, axons from the Th invade specialized regions of the cortex (somatosensory, visual, auditory, motor), and target specific sites within those regions (Dufour, 2003). In selecting specific targets within the NC, Th axons maintain a topographic arrangement: medial Th nuclei project to the medial cortex, and progressively more lateral nuclei project to more lateral cortical regions.

When innervating the cortex, the Th sends axons through an intermediate region in the ventral telencephalon (VTe; or basal ganglia primordium). This region is responsible for an early sorting of TC axons before they are sent out to specialized regions of the cortex. Thus, the VTe plays a key role in controlling the initial topography of Th projections to the NC (for review see Garel & Rubenstein, 2004). In this paper, we explore two mechanisms that contribute to the formation of topographic maps between the Th and NC. The first of these is based on the expression of Eph/ephrin molecules, functions without the depolarization of postsynaptic cells, and is largely responsible for establishing an initial, coarse topographic map. The second mechanism is based on Hebbian-type correlations between the activities of neurons, is mainly responsible for subsequent refinements in topographic projections, and remains active into adulthood. A computational model that integrates these two mechanisms is proposed and tested in simulation experiments involving map development, refinement, and reorganization following focal deafferentation, a localized loss of thalamic input from defined regions of the topographic map.

2. The role of Eph/ephrin molecules in guiding axons

Eph/ephrin complementary molecules are positional labels determined by localized signals in the early embryo that are expressed along a continuous gradient across the Th, VTe, and neocortical regions (see Figure 1). In particular, EphA4 is expressed across the Th, while its complement, ephrin-A5, is found in the VTe and NC. Several *in vitro* studies point to the control of TC maps by Eph/ephrin genes (for a review see Vanderhaeghen & Polleux, 2004). In addition, *in vivo* studies suggest a dual role for the Eph/ephrin complex (Dufour, 2003), controlling both *inter-area* specificity (different sensory modalities to different NC regions) and *intra-area* specificity (arranging axons in a topographically faithful manner within each NC region). Of particular interest is the repellent role attributed to ephrin-A5 in the NC, guiding axons by preventing them from entering erroneous sites.

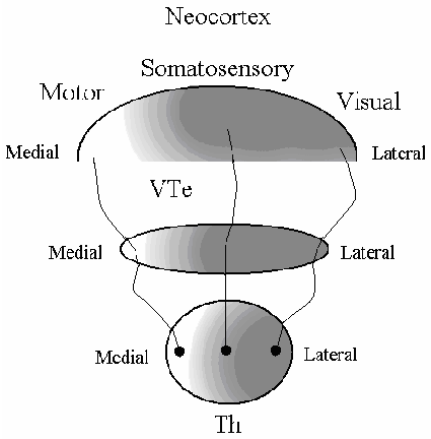

Figure 1. Inervation of TC projections from the thalamus (Th) to the neocortex. The shading shows a gradient of expression of Eph/ephrins. Lines across the regions represent axonal projections.

Previous theoretical and experimental work on non-cortical brain regions has shown that topographically correct initial positions can be obtained without synaptic activity (for a model and review see Thivierge & Balaban 2005). Studies of cortical somatosensory map formation in rodents have also shown that activity-dependent mechanisms are not essential for the development of TC topography (Erzurumlu & Kind, 2001). Activity serves a subsequent role in refining the initial projections; at this later stage, the activity-based process can only provide slight local refinements to the established position of axons.

Interactions between activity-dependent and independent processes are still largely unexplored in cortical neuronal network models. These interactions may explain difficulties in the recovery of neural network function in adult mammals. If a large role is initially played by activity-independent processes, and this role diminishes later in development, leaving adults with activity-based mechanisms that can only produce small-scale changes, this may explain why it is difficult to recuperate from neural disruptions that require large-scale map reorganization.

3. The servomechanism model of axonal guidance

It is reasonable to turn to computer simulations to formalize and integrate theories about cortical map organization and generate novel testable hypotheses. The servomechanism model (Honda, 1998) is a popular model of axonal guidance via Eph/ephrins. It specifies a way in which markers expressed in gradients along a target site guide the growth cones of axons to particular gradient locations. This model was originally designed to explain the dynamic time-course of axonal growth from the retina to the tectum, and the creation of a map between these two regions that conserves topography and polarity (Honda, 1998, 2003; Thivierge & Balaban, submitted).

The servomechanism model is based on the law of mass action. This law provides an equation for computing the "topographic signal" G emerging from the interaction of receptor concentration $R(\cdot)$, and ligand concentration $L(\cdot)$. Allowing for multiple receptors $R_i(u)$ and ligands $L_j(v)$, with promiscuous interactions between them, the concentration $G(u,v)$ of topographic signal within an axon originating from a start position u (e.g., in the Th) when it is at end position v (e.g., in the VTe) is given by a second order kinetic equation:

$$G(u,v) = \sum_{i,j} h_{ij} R_i(u) L_j(v), \tag{1}$$

where h_{ij} is a constant scaling factor. The receptor concentrations are functions of the Eph/ephrin molecular gradients. In all simulations reported, the following gradients were employed:

$$\begin{aligned} R(u) &= 1/1 + e^{u}, \\ L(v) &= 1/1 + e^{v}. \end{aligned} \tag{2}$$

Axons travel through a target region until a “stop signal” is produced to cease migration. According to a local optimum rule, a stop signal is determined by local minimum: $\partial G(u,v)/\partial v \cong 0$. This is obtained by determining the gradient of $G(u,v)$ for a given target location v:

$$\frac{\partial G(u,v)}{\partial v} = R_1(u) \frac{\partial L(v)}{\partial v}. \tag{3}$$

Migration in performed in random steps Z. It is biased towards progressing forward by making $Z = (1 + Q) / 2$, where Q is obtained according to the gradient of $G(u,v)$:

$$Q = \eta \frac{\partial G(u,v)}{\partial v}, \tag{4}$$

where η is a parameter regulating the step-size of the migration.

This migration process is mediated by the fact that axons will likely avoid a region of high density and favor a neighboring site on the target. This is incorporated in the model by the addition of axonal competition (Honda, 2003; Thivierge & Balaban, 2005).

Because the initial servomechanism model was designed to address migration in the retinotopic system, some modifications must be made if we are to model TC projections: (1) there is an intermediate site of projection in the VTe; (2) TC projections display inter-site as well as intra-site topography.

Below is a step-by-step process of migration for one axon, along a dimension x (the same process applies to other dimensions, and migration along each dimension is independent of other dimensions). In addition, because TC projections will migrate through an intermediate target site in the VTe, this process is repeated twice: (1) between the Th and VTe; and (2) between the VTe and S1. Hence, the ligand function $L(\cdot)$ of the target site becomes the receptor function $R(\cdot)$ of the sending site when the process is repeated. In principle, it would be possible to add many intermediate sites of projections iteratively to produce a more realistic model of axonal guidance through several regions of the brain. The description below is meant to be as general as possible to reflect this idea.

Step 1. Initialization stage.

a) define unit migration of the projecting cone in random steps along the x dimension: $(1+Q_x)/2$, where Q_x is a random number constrained to be $0 < Q_x < 1$.

b) define two neighboring sites at random in the target region, j and j+1.
c) set n_c, a constant defining the critical population density at a given site.
Step 2. Migration stage.

a) compute distance at the start position: $d_1^{start} = (R_1(u)L_1(v) - M)^2$, and distance at the end position: $d_1^{end} = (R_2(u)L_2(v) - M)^2$, where M is the maximum receptor saturation.
b) compute repulsiveness of start location as $r^{start} = (R_1(u)L_j(v) - M)^2$, and repulsiveness of end position as $r^{end} = (R_2(u)L_j(v) - M)^2$.
c) if $d_1^{start} > d_1^{end}$, then the axon moves to d_1^{end}, according to $p^{end} / (p^{end} + p^{start})$ where $p^{start} = p^{start}(d_1)$, $p^{end} = p^{start}(d_1^{end})$, and p is a Gaussian function mediating the size of migration. Otherwise it does not move.
Step 3. Axonal competition.
If repulsiveness of the end location is lower than start location, i.e., $r^{end}<r^{start}$, and if j or j+1 has larger density than n_c, the axon migrates from the site of higher density to the site of lower density.
Repeat steps 1-3. Repeat for a given number of steps, or until a termination site is reached, i.e., if d is sufficiently close to zero ($d \cong 0$).

The η parameter of Eq.4 controls the amount of branching of the model, as well as velocity of migration; a higher value of η leads to less branching (i.e., less dendritic formation) and faster progression of axons (Thivierge & Balaban, submitted). Default parameters for all simulations in this work are provided in Table 1.

Table 1. Default parameters of the Hebbian servomechanism model

Activity-independent parameters	Activity-dependent parameters
critical population density: $n_c = 20$	maximum spine saturation: $s_j = 100$
maximum receptor saturation: $M = 100$	spine growth rate: $\lambda = 0.08$
step-size of migration: $\eta = 0.1$	spine depletion rate: $\phi = 0.02$
number of iterations: 100	number of iterations: 100
scaling factor: h_{ij}=1.0	

4. In vivo inter-area neocortical guidance

Competitive servomechanical guidance of TC axons was used to simulate results of experiments with ephrin-A5 knockout mice (see Figure 2, and Vanderhaeghen, 2000; 2004 for a discussion). In ephrin-A5 knockout mice, gene disruption causes topographic distortions of projections to the NC. Specifically, medial neocortical regions are contracted, and lateral regions expanded, changing the size of cortical projection areas up to 50%. Despite this shift, a roughly correct topography is maintained. These results can be accounted for by a lateral shift of TC axons in the VTe. In knockout mice, ventral Th axons are no longer limited to the medial VTe, and also travel to lateral regions of this intermediate target (Dufour et al., 2003). The surplus of lateral axons in the VTe goes on to innervate the lateral regions of the cortex. Axons are eventually forced out of this “overprojected” region by competitive processes, and start invading the medial portion of the cortex. In sum, an increase in the number of projections to the lateral cortex leads to a lateral expansion of the cortex, in turn leading to a contraction of the medial cortex.

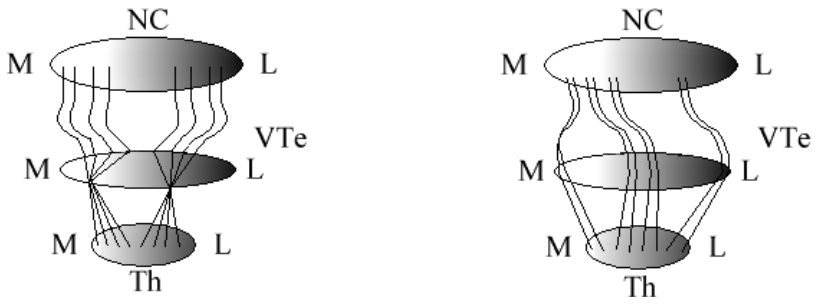

Figure 2. Simulation of Vanderhaeghen (2000). Servomechanical innervation of TC projections. M=medial; L=lateral; Th=thalamus; VTe=ventral telencephalon; NC=neocortex. (a) normal innervation; (b) disrupted ephrin-A5 in the VTe of knock-out mice. The Th in this model is a a 25x25 grid. 8 axons were sent out, uniformly covering the thalamus from medial to lateral: u_i={2,5,8,11,14,17,20,23}.

5. Activity-dependent processes

The model described in the previous section was upgraded to include activity dependent mechanisms of cortical map organization and maintenance. The role of neural activity in the refinement and maintenance of cortical maps is well established (Katz & Shatz, 1996), but the way that activity-dependent processes interact with activity-independent processes during cortical map formation are not well understood, indicating a need for models that combine activity-independent and dependent processes.

5.1 NMDA and GABA receptors. Our model incorporates excitatory NMDA (N-methyl-D-aspartate) and inhibitory GABA (gamma-aminobutyric acid) receptors. Activity-dependent plasticity and synapse formation often utilize NMDA glutamate receptors, because of their role in controlling the entry of Ca^{2+} into the postsynaptic cell (Helmehen, 2002). In order to allow the retraction and pruning of axonal connections, we combine NMDA excitation with signaling via GABA receptors, which inhibit the cell via current shunting and hyperpolarisation, and thus can reduce synaptic efficacy.

5.2 Hebbian learning. Our proposed model is based on Hebbian learning. According to this form of synaptic plasticity, connections get strengthened by synchrony of firing between sending and target neurons. Because our model does not include temporal dynamics, activity is represented during discrete update intervals. In this context, presynaptic and postsynaptic neurons will be said to fire in synchrony if, at a given time, when the presynaptic neuron is active, the postsynaptic neuron is also active. Hebbian plasticity reflects the coincidence-detection function of NMDA receptors, requiring both presynaptic activity (glutamate release) and postsynaptic activity (depolarization) for channel-opening.

5.3 Winner-take-all. The type of Hebbian plasticity we employ features a winner-take-all rule, meaning that each postsynaptic target neuron will ultimately receive activation from a single presynaptic projecting neuron. This mechanism is meant to reflect the idea of competition for a resource (i.e., a trophic substance) available in limited quantity in the target. Thus, the initial surplus of connections will eventually get pruned out.

Competitive Hebbian models lead to some of the best accounts of map organization from a developmental perspective in the visual cortex (Erwin, Obermayer, & Schulten, 2001). Because similar models have been applied to the somatosensory cortex (Sklar, 1990; Goodall et al., 1996; Benuskova et al., 1999; Song & Abbott, 2001), the conclusions of Erwin et al. may also apply to the somatosensory maps under study in the current work. Winner-take-all rules are also biologically plausible with respect to somatosensory maps. At the end of the activity-dependent process, the projecting neuron that forms the

most synapses “wins” the right to innervate that target. Thus, the activity-dependent process can be viewed as a form of competition for exclusive “ownership” of the target. Winner-take-all rules are plausible with respect to somatosensory maps. At the end of the activity-dependent process, for each target neuron, the sending neuron with the most dendritic projections wins the representation of that target. Thus, the activity-dependent process can be viewed as a form of competition for exclusive “ownership” of the target.

5.4 Dendritic spine formation. The strengthening of connections between neurons is reflected in dendritic spine formation on the target neuron. Dendritic spines are small thorn-like structures that receive excitatory input. Spine formation is thought to underlie synaptic plasticity and perhaps long-term memory formation (Klein, 2004).

5.5 Continued influence of Eph/ephrins. A large corpus of research argues that molecules involved in axonal guidance during embryonic development can be reused in adulthood, both to complete developmental processes, to adapt to changing environmental demands, or to re-establish the functional integrity of neuronal circuits following injury (Aubert et al., 1995).

5.6 Formal description. This is a population model with average firing rate, excluding temporal dynamics. In this model, a sending axon i will grow a number of spine formations w_{ij} on a target neuron j according to a winner-take-all Hebbian rule. Activation y passing through each axon is:

$$y_{ij} = w_{ij} x_i , \tag{5}$$

where x_i is input activation according to $0<x_i<1$. Activation a_j of a target neuron is computed as:

$$a_j = \sum_j y_{ij} \ . \tag{6}$$

The number of spines on a target is updated according to:

$$\Delta w_{ij} = \lambda \left(x_i - \left(w_{ij} / s_j \right) \right), \tag{7}$$

where s_j is the maximum number of spines possible and λ is a free parameter controlling the growth rate of spines. A winner-take-all rule is applied as follows:

$$w_{ij}^t = \begin{cases} \left(w_{ij}^{t-1} - \phi \right) + \Delta w_{ij}^t & \text{if } y_{ij} = \max_j \left(y_{ij} \right) \text{ and } w_{ij}^t \geq \phi \\ w_{ij}^{t-1} - \phi & \text{if } w_{ij}^t \geq \phi \\ 0 & \text{otherwise} \end{cases} \tag{8}$$

where t is an iteration of the algorithm, and ϕ is a free parameter controlling the depletion rate of spines. With this update rule, we impose a strict limit of 0 on the minimum of w_{ij}. It is important to insure that $\phi < \lambda$, so that inhibition does not prevent the winning target from gaining spines, but still decreases the number of spines in other sites. With the activity-dependent mechanism, we add one extra step to the activity-independent model of the previous section:

Step 4. Activity-dependent stage. Update dendritic spine formation according to Eq. 8.
Repeat steps 1 through 4. Repeat the activity independent (1 and 2) and activity dependent (3) steps, each for a predetermined number of iterations.

With the addition of the activity-dependent process, our goal is to model the intra-area sorting of TC axons. Thus, for our purposes, the only plastic links are between the VTe and NC. The Th links are set to "1". This means that the update rules in Eq. 7-8 apply only to connections between the VTe and S1. In order to understand the behavior of the model, we will report on the relative density of dendritic spines going from each projecting neuron to each target neuron. This mass of dendritic spines will be referred to as the "spine landscape". The initial spine landscape is fully determined by the activity-independent process, but is reshaped with activity, as the following simulations will demonstrate.

6. Intra-area S1 guidance

In this section, we show refinements in axonal projections through a combination of activity-dependent and independent mechanisms. We model the refinements that occur within a specific region of NC, rather than across several regions (the model in Section 4 above), assuming that inter-area topography is mainly established through development by activity-independent guidance cues, while intra-area topography is formed at later stages and involves both activity-dependent and independent processes. We restrict this account to models based on regeneration experiments in the somatosensory (S1) neocortical region (Figure 3). For all simulations that follow, we first run the activity-independent process (steps 1-3) followed by the activity-dependent process (steps 1-4), each for 100 iterations. The dendritic spine landscape obtained by the activity-independent process alone is generated by sending a large number of axons from each start location (as many for each projecting neuron as there are sites in the target region).

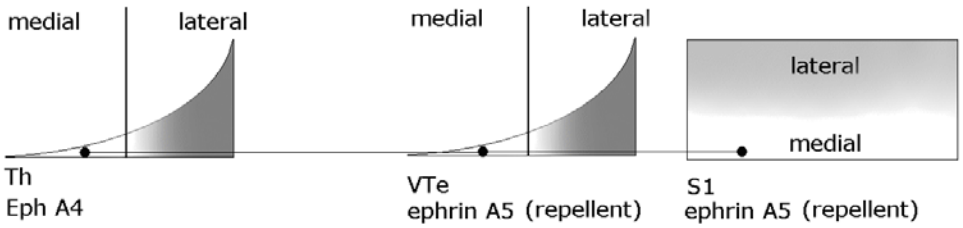

Figure 3. Inervation of the somatosensory cortex. The shading shows gradients of Eph/ephrin expression.

6.1 Spine formation around a single cell. Guidance of three projecting axons onto a single target is shown in Figure 4a. (one that forms 4 synapses, one with 3 synapses, and one with 2 synapses). This figure shows the distribution of dendritic spines for a given target. As depicted, synapses tend to

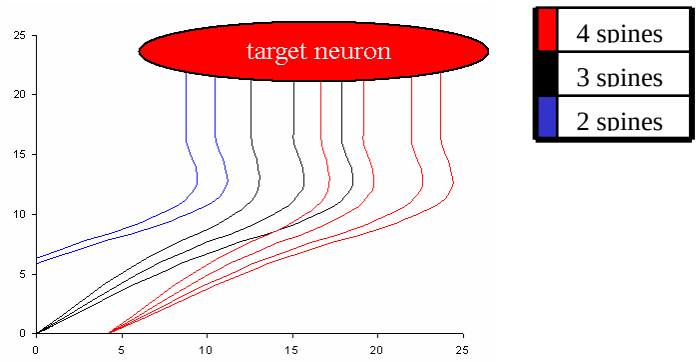

(a)

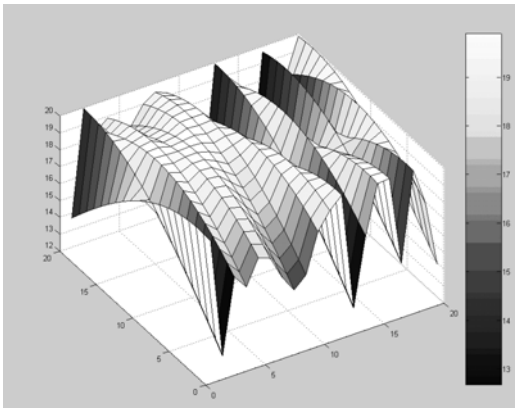

Figure 4. (a) Evolution of a single target. In this simulation, u_i={9,12,24} on 25x25 topographic grids in the Th, VTe, and NC. (b) Initial spine landscape projecting on two dimensions of the S1 neocortex. 20x20 topographic grids were used on the Th, VTe, and NC; 20 axons were projected for each Th location, totaling 8000 axons.

distribute themselves evenly with respect to the target neuron. This is due to the activity-independent competitive mechanisms that force synapses to move away from sites of high density. Synapses from the same projecting neuron also generally tend to cluster together.

6.2 Initial spine landscape. After the activity-independent process, the initial dendritic landscape resembles Gaussian columns centered on the termination points of axons (see Figure 4b). For a given projecting neuron, the winning sites have more dendrites, and surrounding sites less; distant sites have none or nearly none.

6.3 Activity-dependent refinement. With the current model, it is possible to illustrate the evolution of a dendritic landscape for a single target neuron. This allows us to assess the impact of activity-dependent processes on the growth and retraction of projections initially formed by the activity-independent processes alone (Figure 5). The winning neuron attains an asymptotic value near 100 spines at the end of 100 iterations.

Prior to activity dependent processes, there is a dense mapping, where many projecting axons from the VTe innervate each single target in S1. However, through a combination of activity-dependent and independent processes, only one of these projecting neurons is strengthened by the addition of spines, while other neurons retract their initial connections to the target.

7. Regeneration experiments with local area expansion

This section replicates experiments in primates showing an expansion of the representation of regions near a site of ablation of projections (Merzenich et al., 1984). Studies utilizing MEG recordings in surgically amputated human adults showed similar results (Mogilner et al., 1993).

7.1 Unmasking. Cortical reorganization following neural deafferentation is based on the principle of neural *unmasking* (Figure 6a). Initially, projecting neuron #2 dominanates the input to the target neuron because of its high spine density. If this link is disrupted, the weak connections from projecting neurons #1 and #3 will receive more spines from the target neuron. This growth will shift the input sensitivity of that target neuron. In the end, whichever projecting neuron has the highest number of dendritic spines on the target neuron gets to determine the representation of that target.

7.2 Reorganization following focal deafferentation. After ablation (i.e., deafferentation) of a small region of sensory input, a reorganization of the dendritic landscape occurs (Figure 6b), characterized by regions at the periphery of the ablation taking over the representation of the target neuron.

Ablation of a small portion of the sensory surface leads to a characteristic reorganization of axons on the target region. Figure 7 illustrates the cortical representation of two “patches” that can be interpreted as fingers, before and after ablation. Prior to ablation, each finger is represented by roughly half of the

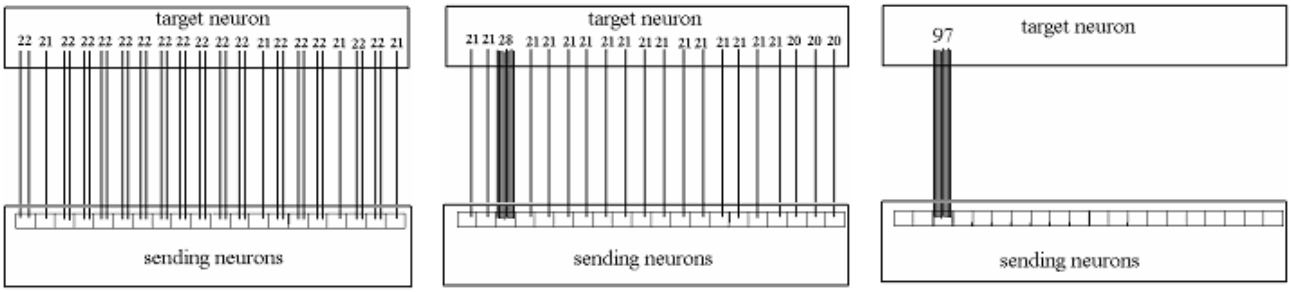

t=1 *t*=2 *t*=100

Figure 5. Evolution of dendritic arborisation for a single target. Shows retraction and death versus expansion of innervation for winner. 20 Th neurons (each with 20 connecting axons) were projected onto a single target neuron in the NC. The projecting sites were equally spaced: u_i={1,2,...,20}.

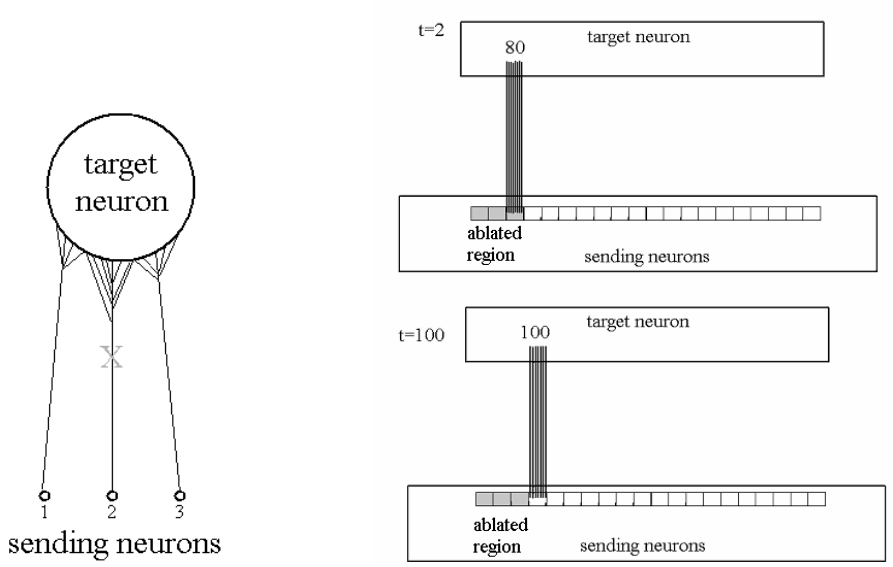

(a) (b)

Figure 6. (a) The unmasking phenomenon. (b) Reorganization following ablation. reaches asymptote at 100. 20 Th neurons (each with 20 connecting axons) were projected onto a single target neuron in the NC. The projecting sites were equally spaced: u_i={1,2,...,20}.

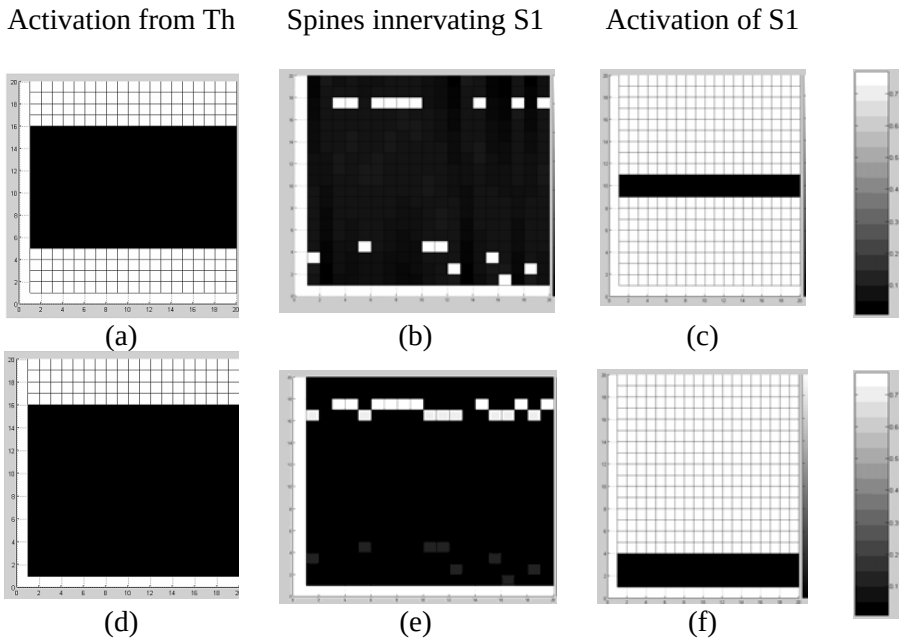

Figure 7. Ablation or complete sensory depravation of a finger surface. (*a*) Input stimulation of two fingers; (*b*-*c*) Finger representations before ablation. Finger 1 inherits 45% of the available S1 surface; finger 2 inherits 40% of this surface. (d) Input stimulation after ablation of finger 2. (e-f) after ablation or significant reduction in activity. Finger 1 expands to 85% of the S1 surface, and finger 2 is completely eliminated. *b* and *e* represent dendritic landscape, while *c* and *f* represent S1 surface. 20 Th neurons (each with 20 connecting axons) were projected on the NC. The projecting sites were equally spaced: u_i={1,2,...,20}.

cortical surface. Following ablation of one finger and subsequent reorganization, the remaining finger now represents most of the available cortical surface.

7.3 Sensory deprivation. The proposed Hebbian model is sensitive to the probability distribution of activity across different projections. Thus, a large difference (i.e., complete neural deafferentation) can be captured, but a small difference (i.e., reduced stimulation) can also lead to map reorganization. To demonstrate this, we reduced the stimulation to one artificial finger but not the other (Figure 8). Dendritic spines are either fully maintained, or fully pruned; a stimulation of at least x=0.3 (i.e., 30% preferential activation) guarantees that connections are maintained. Hence, a certain threshold of differential stimulation (here about a 70% difference) to neighboring fingers is needed before one sees changes in map organization. This prediction of the model for a threshold effect of differential stimulation on map reorganization is interesting for future experimental assessment.

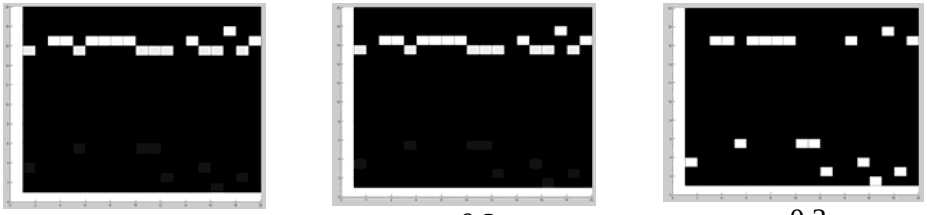

Figure 8. Different degrees of preferential sensory deprivation to one finger. The x values represent the input stimulation provided to the deprived finger, while the other finger always received full stimulation (x=10). 20 Th neurons (each with 20 connecting axons) were projected onto the NC. The projection sites were equally spaced: u_i={1,2,...,20}.

7.4 Continued influence of activity-independent processes. The model indicates that the activity-independent process maintains some influence over the organization of cortical maps into adulthood. Figure 9 shows a simulation involving ablation of a section located in the center of a topographic map. Without an activity-independent process, the activity-dependent process re-distributes connections on both sides of the lesion (Fig.9c). However, with the influence of the activity-independent process, all synapses get shifted to the same side of the lesion (Fig.9d).

In this simulation, the activity-dependent process provides information about which sections of the map need to be reorganized, while the activity-independent process is mainly responsible for organizing the new dendritic landscape. Experiments with neural deafferation in monkeys (Pons et al., 1991) reported

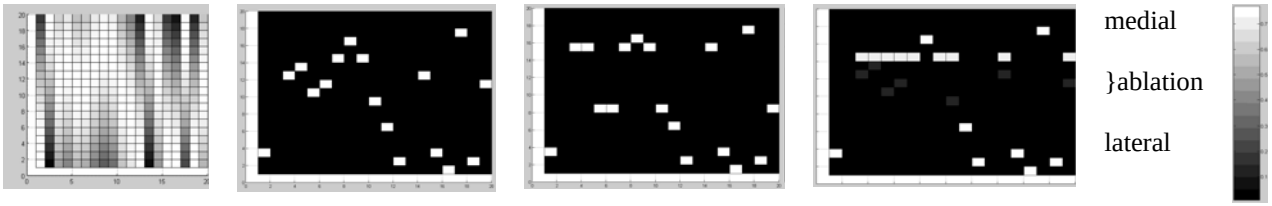

Figure 9. Influence of activity-independent processes in cortical reorganization following ablation. (a) Initial dendritic landscape after 100 iterations of the activity-independent process; (b) Before ablation (c) Without the activity-independent process. (d) Addition of an activity-independent mechanism guided by an Eph molecular gradient on the Thalamus expressed in a high-low fashion from medial to lateral regions. 20 Th neurons (each with 20 connecting axons) were projected onto the NC. The projecting sites were equally spaced: u_i={1,2,...,20}.

that S1 reorganization was characterized by an expansion of regions that "stretched out" medially (i.e., directionally). Our model suggests that these findings may be the result of activity-independent guidance cues still active in adult animals.

9. Discussion

We propose a unified model of cortical sensory map formation and adult plasticity that includes the continued influence of both activity-independent and activity-dependent mechanisms. This model can account for initial map development in normal and knock-out mice, as well as activity-dependent refinements in topography and reorganization following ablation or sensory depravation in adulthood.

We argue that the activity-independent process guides the establishment of the target-winning sites. In the case of map disruption, the activity-dependent mechanisms will help guide the reorganization. However, activity-independent mechanisms still play a crucial role in this reorganization process. As shown in Figure 9, activity-independent processes may play a role in controlling the direction of expansion following a focal deafferentation. Although past research on modeling somatosensory map formation has acknowledged the importance of initial (i.e., activity-independent) conditions in training thalamocortical maps (Song & Abbott, 2001), none has proposed a mechanisms for this pre-wiring.

In the current study, we propose a biologically plausible way in which activity-independent mechanisms may contribute to synaptic plasticity far into adulthood. With this approach, we have replicated results of a classic study by Pons (1991) in which S1 neurons from a deafferated region relocated medially. In light of the new approach, we may be able to revisit several experimental findings of map reorganization. Thus, interestingly, we may be in a position to reinterpret results that were found a number of years before the role of Eph/ephrin molecular guidance was well understood.

The current study underlines several implications for modelling learning and development. Firstly, we provide arguments to the effect that models of learning that start out random are not biologically plausible. Rather, there are genetically-determined contraints on the connectivity of maps prior to any activity-dependent process. Secondly, our account demonstrates why the brain requires massive pruning, as has been reported in childhood (Innocenti, 1995), the reason being that genetically determined markers produce maps that are over-connected.

9.1 Alternative accounts.

Other models have addressed various results associated with somatosensory map plasticity (Grajski & Merzenich, 1990; Sutton, 1994; Sklar, 1990; Goodall et al., 1996; Benuskova et al., 1999; Song & Abbott, 2001). However, these models require the random initialization of connection weights, a biologically unrealistic feature that does not take into account the formation of topographically faithful maps prior to activity-independent processes.

Several other models have accounted for the influence of Eph/ephrins in the development of the visual system (e.g., Honda, 2003; Thivierge & Balaban, 2005). However, the role of these molecules appears to extend to other domains of map formation that have not yet been modeled, including the hippocampus/entorhinal cortex and the vomeronasal system. Future work should be directed to the study of those systems.

9.2 Summary.

This research makes the following contributions: (1) a model combining activity-dependent and independent mechanisms for initial guidance of thalamocortical axons forming sensory maps in the cortex and continued plasticity of these structures; (2) the application of the same model to both embryonic stages and adulthood, including reorganization following ablation; (3) the inclusion of both intra-area and inter-area topography in a single model; (4) addition of an iterative structure to the servomechanism model of axonal guidance, allowing it to be applied to sequential projection decisions; (5) simulation of in-vivo results involving knockout of ephrin-A5; (6) simulation of reorganization experiments involving expansion; and (7) generation of new hypotheses concerning the interaction of activity-dependent and independent processes. For instance, the model predicts that there should be a threshold of differential stimulation between neighboring sites required for somatosensory map

reorganization (here a change of about 70%), and as well as predicting the directional characteristics of map reorganization following ablation.

Acknowledgements
This research was supported by a scholarship from FCAR to J.P.T., and a grant from NSERC to T.R.S.

References

Aubert, I., Ridet, J.L., & Gage, F.H. (1995) Regeneration in the adult mammalian CNS: Guided by development. *Curr. Opin. Neurobiol., 5*, 625–635.

Benuskova, L, Ebner, F.F., Diamond, M.E., & Armstrong-James, M. (1999). Computational study of experience dependent plasticity in adult rat cortical barrel-column. *Network: Computation in Neural Systems, 10*, 303-323.

Dufour, A., et al. (2003). Area specificity and topography of thalamocirtical projections are controlled by ephrin/Eph genes. *Neuron, 39*, 453-465.

Erwin, E., Obermayer, K., & Schulten, K. (2001). Models of orientation and ocular dominance columns in the visual cortex: A critical comparison. In: Self-Organization Map Formation: Foundations of Neural Computation. K. Obermayer and T.J. Sejonowski (Eds). MIT Press.

Erzurumlu, R.S., & Kind, P.C. (2001). Neural activity: Sculptor of 'barrels' in the neocortex. *Trends Neurosci. 24*, 589–595.

Garel, S., & Rubenstein, J.L.R. (2004). Intermediate targets in formation of topographic projections: Inputs from the thalamocortical system. *Trends in Neuroscience, 27*, 533-539.

Goodall, S., Reggia, J.A., Yinong, C., Ruppin, E., & Whitney, C. (1996). A computational model of acute focal cortical lesions. *Stroke, 28*, 101-109.

Goodhill, G.J. (1998). Gradients for retinotectal mapping. Advances in Neural Information Processing Systems, 10, 152-158.

Grajski, K., & Merzenich, M. (1990). Hebb-type dynamics is sufficient to account for the inverse magnification rule in cortical somatotopy. *Neural Comp, 2*, 71-84.

Honda, H. (2003). Competition between retinal ganglion axons for targets under the servomechanism model explains abnormal retinocollicular projection of eph receptor-overexpressing or ephrin-lacking mice. *J. Neurosc., 23*, 10368-10377.

Katz, L.C., & Shatz, C.J. (1996). Synaptic activity and the construction of cortical circuits. *Science, 274*, 1133–1138.

Klein, R. (2004). Eph/ephrin signaling in morphogenesis, neural development and plasticity. *Current Opinion in Cell Biology, 16*,580-589.

Merzenich, M.M., Nelson, R.J., Stryker, M.P., Cynader, M.S., Schoppmann, A., & Zook, J.M. (1984). Somatosensory cortical map changes following digit amputation in adult monkeys. *J Comp Neurol, 224*, 591-605.

Miranda, J.D., White, L.A., Marcillo, A.E., Willson, C.A., Jagid, J., & Whittemore, S.R. (1999). Induction of Eph B3 after spinal cord injury. *Exp. Neurol., 156*, 218–222.

Mogilner, A., Grossman, J.A.I., Ribary, U., Joliot, M., Volkmann, J., Rapaport, D., Beasley, R.W., & Llinas, R.R. (1993). Somatosensory cortical plasticity in adult humans revealed by magnetoencophalography, *Proc. Natl. Acad. Sci. USA, 90*, 3593-3597.

Palmer, A., & Klein, R. (2003). Multiple roles of ephrins in morphogenesis, neuronal networking, and brain function. *Genes and Development, 17*, 1429-1450.

Sklar, E. (1990). A simulation of somatosensory cortical map plasticity. *Proc. of IEEE International Joint Conference on Neural Networks*, 727-732.

Song, S., & Abbott, L.F. (2001). Cortical development and remapping through spike timing-dependent plasticity. *Neuron, 32*, 339-350.

Stein,, E., Savaskan, N.E., Ninnemann, O., Nitsch, R., Zhou, R., & Skutella, T. (1999). A role for the Eph Ligand Ephrin-A3 in entorhino-hippocampal axon targeting. *Journal of Neuroscience, 19*, 8885-8893.

Sutton, G, Reggia J, Armentrout S, and D'Autrechy C (1994). Map Reorganization as a Competitive Process, *Neural Computation*, 6, 1-13.

Thivierge, J.P., & Balaban, E. (2005). Hebbian-based Servomechanical Guidance with Local Optimal Rules. *IEEE International Joint Conference on Neural Networks*, in press.

Thivierge, J.P., & Balaban, E. (submitted). Servomechanical guidance with local optimum rules and axonal competition. *Neurocomputing*.

Vanderhaeghen, P., et al. (2000). A mapping label required for normal scale of body representation in the cortex. *Nat. Neurosc., 3*, 358-365.

Vanderhaeghen, P., & Polleux, F. (2004). Developmental mechanisms patterning thalamocortical projections: Intrinsic, extrinsic and in between. *Trends in Neuroscience, 27,* 384-391.